

# ASSESSMENT OF FIRED RED CLAY CERAMICS WITH ORE TAILINGS FOR CONSTRUCTING ARTIFICIAL REEF STRUCTURES AT DIFFERENT SINTERING TEMPERATURES

Marilou E. Legaspi<sup>a,\*</sup>, Christian D. Calleno<sup>b,c</sup>, Edison A. Limbaga<sup>a,c</sup>, Lori-Ann I. Cabalo<sup>a,c</sup> and Liezl M. Jabile<sup>a,c</sup>

<sup>a</sup>Advanced Porous Ceramic Particles (APCerP) Lab., Ceramic Researches for Engineering Advanced Technology & Environment (CREATE) Lab, Research Center for Advanced Ceramics (RCAC), Research Institute for Engineering and Innovative Technology (RIEIT), Mindanao State University – Iligan Institute of Technology, Iligan City, Philippines

<sup>b</sup>Environmental Science Graduate Program, School of Interdisciplinary Studies, Mindanao State University – Iligan Institute of Technology, Iligan City, Philippines

<sup>c</sup>Department of Materials and Resources Engineering and Technology, College of Engineering, Mindanao State University – Iligan Institute of Technology, Iligan City, Philippines

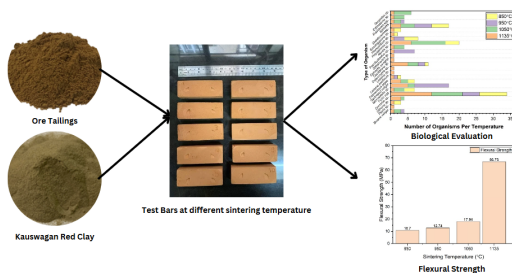
<sup>d</sup>Technology Application & Promotion Unit, Office of the Vice Chancellor for Research & Enterprise, Mindanao State University – Iligan Institute of Technology, Iligan City, Philippines

## Article history

Received  
19 November 2024  
Received in revised form  
23 April 2025  
Accepted  
19 June 2025  
Published online  
28 February 2026

\*Corresponding author  
marilou.legaspi@g.msuit.edu.ph

## Graphical abstract



## Abstract

This study investigates the influence of sintering temperature on the biological performance of ceramic test bars exposed to marine environments. Four sintering temperatures—1135°C, 1050°C, 950°C, and 850°C—were evaluated by deploying test bars in a Marine Protected Area (MPA) and analyzing the number and types of organisms that adhered to their surfaces. The results revealed a clear trend, with the test bars sintered at 1135°C showing the highest biofouling activity, recording a total of 54 organisms. As the sintering temperature decreased, the number of organisms declined, with 49 organisms on the 1050°C sample, 35 organisms on the 950°C sample, and 33 organisms on the 850°C sample. These findings suggest that higher sintering temperatures, which result in denser and smoother surfaces, promote greater biofouling, while lower sintering temperatures may hinder organism attachment. This study provides valuable insights for optimizing material properties for marine applications, for the application of coral reef preservation.

**Keywords:** artificial reef, ceramic test bars, sintering, biological performance

© 2026 Penerbit UTM Press. All rights reserved

## 1.0 INTRODUCTION

The depletion and degradation of natural coral reefs, driven by climate change, overfishing, pollution, and destructive human activities, pose significant threats to marine ecosystems worldwide[1]. Coral reefs, often referred to as the "rainforests

of the sea," provide critical habitats for a diverse range of marine species, contribute to shoreline protection, and support fisheries and tourism industries[2]. However, as these natural ecosystems decline, the need for artificial reef structures has become increasingly important. Artificial reefs, which mimic the structure and function of natural reefs, offer an alternative

solution to promote marine biodiversity, restore ecological balance, and rehabilitate damaged reef systems[3].

Traditionally, artificial reefs have been constructed using materials such as concrete, steel, and limestone due to their availability and durability in underwater environments[4]. However, these materials often present limitations such as environmental impact, high cost, and limited suitability for certain marine ecosystems. In recent years, there has been a growing interest in exploring more sustainable and ecologically compatible materials for artificial reef construction[5]. One promising alternative is the use of fired red clay ceramics combined with ore tailings, which offers a low-cost, environmentally friendly solution with potential for enhanced material properties.

Ore tailings, the by-products of mining and mineral processing activities, represent a significant environmental challenge. Large quantities of tailings are often stored in waste impoundments or discarded, leading to contamination of water bodies, soil degradation, and adverse effects on surrounding ecosystems[6]. Repurposing ore tailings in construction applications not only reduces the environmental footprint of mining operations but also supports circular economy principles by transforming industrial waste into valuable resources[7]. When integrated with red clay ceramics, ore tailings may contribute to improving the structural integrity and ecological functionality of artificial reef structures, offering a novel approach to sustainable reef construction[8].

Red clay ceramics, known for their high compressive strength, low permeability, and resistance to marine conditions, are widely used in various civil engineering applications[9]. The use of fired ceramics in artificial reef construction can create robust, durable structures that withstand the harsh marine environment while supporting the settlement of marine organisms such as corals and algae[5]. However, the properties of fired ceramics, including porosity, strength, and microstructure, are highly dependent on the sintering process. Sintering, which involves heating powdered materials below their melting point, plays a crucial role in controlling the material's mechanical and physical characteristics[10].

Research has shown that varying the sintering temperature can significantly influence the porosity, density, and strength of ceramics, with higher temperatures generally leading to denser and stronger materials[10-12]. In the context of artificial reefs, optimizing the sintering temperature is essential for achieving the desired balance between structural durability and ecological functionality[13]. Reef structures need to be strong enough to withstand ocean currents and wave action while maintaining sufficient porosity to allow water flow and the attachment of marine organisms[14]. Understanding the impact of sintering temperature on these properties will be key to designing artificial reefs that promote long-term ecological sustainability and resilience in marine environments.

This study aims to assess the feasibility of using fired red clay ceramics mixed with ore tailings for the construction of artificial reef structures. By analyzing the effects of different sintering temperatures on the material properties, including porosity, compressive strength, and durability, this research seeks to identify optimal processing conditions for creating robust and ecologically viable reef structures. Additionally, the study will explore the potential ecological benefits of these materials, focusing on how their physical properties influence

the settlement of marine organisms and the overall health of the artificial reef. The findings of this research will contribute to the growing body of knowledge on sustainable materials for marine ecosystem restoration and provide practical insights for the design and implementation of artificial reefs that address both ecological and environmental challenges.

## 2.0 METHODOLOGY

The Kauswagan Red Clay (KRC) and Ore Tailings were obtained from Kauswagan, Lanao del Norte, Philippines and T'boli. The raw materials were crushed and sieved using a 100 mesh Tyler sieve in 149 microns for initial characterization. The chemical composition of the materials was obtained by Energy Dispersive X-ray Fluorescence (XRF) spectroscopy following ASTM E1621 – 20. The mineralogical composition and crystalline phases were observed by X-ray Diffraction using XRD (Rigaku MiniFlex 600 Dual Wavelength X-ray Diffractometer, CuK $\alpha$ , 40kV). The thermal stability and phase changes of each raw material was analyzed by thermogravimetry-differential thermal analysis (TG-DTA) TG-DTA; TG/DTA300 SSC 5200H, Seiko Instrument, Inc. using air at a gas flow rate of 200mL/min at 10°C/min. The percent composition of the soft mud batch for the formulation was calculated using ultimate proximate analysis. The test bars were fabricated via semi dry pressing method using a metal mold. The sample test bars were air dried for 24 hours, soaked in the oven for 6 hours and fired at the furnace for 4 hours under 4 different temperatures; 850, 950, 1050 and 1135°C. Physical properties such as bulk density, water absorption and apparent porosity were conducted prior to deployment. The flexural strength of the test bars was measured as well before the deployment using a Universal Testing Machine (UTM). The deployment site is in a Marine Protected Area (MPA) at Linamon, Lanao del Norte. After 4 weeks of deployment, the samples were evaluated for biocompatibility.

## 3.0 RESULTS AND DISCUSSION

The XRF data (Table 1) shows that KRC is predominantly composed of silica (SiO $_2$ ), alumina (Al $_2$ O $_3$ ), and iron oxide (Fe $_2$ O $_3$ ), with respective concentrations of 42.66%, 31.46%, and 23.03%. These oxides are essential for enhancing the mechanical strength and thermal stability of the ceramic material when used in structural applications. Silica contributes to the rigidity and durability of the material[15], while alumina is known for improving the hardness and melting point of ceramics[16], making it ideal for use in the harsh conditions of marine environments. The high iron oxide content also suggests a potential for good structural integrity and distinctive coloration, which is typically associated with ceramics made from iron-rich clays[17]. The trace amounts of TiO $_2$  (2.18%) enhance the UV resistance and weathering properties of the material, further supporting its long-term durability in underwater applications[18].

In contrast, the ore tailings show a significantly higher concentration of silica (62.50%) and a lower amount of alumina (14.25%) and iron oxide (7.99%). This suggests that while the

ore tailing alone may not exhibit the same level of mechanical strength as KRC, their high silica content can provide complementary benefits when mixed with KRC, contributing to overall strength and stability. Additionally, the presence of  $K_2O$  (7.67%) and  $Na_2O$  (1.78%) in the ore tailings highlights their potential role as fluxing agents. These alkali oxides lower the sintering temperature of the mixture, promoting the densification process during firing, which is essential for producing compact, durable ceramics with reduced porosity[10]. These fluxing agents, while beneficial for processing, must be carefully balanced to avoid excessive vitrification, which can lead to brittleness or diminished porosity, impacting the material's ecological performance in reef structures[11].

**Table 1** Oxide Analysis of Kauswagan Red Clay (KRC) and Ore Tailings

Oxides	Composition (%)	
	KRC	Ore Tailings
$SiO_2$	42.66 %	62.50 %
$Al_2O_3$	31.46 %	14.25 %
$Fe_2O_3$	23.03 %	7.99 %
$TiO_2$	2.18 %	0.56 %
$CaO$	0.15 %	1.43 %
$SO_3$	0.14 %	2.02 %
$V_2O_5$	0.11 %	0.05 %
$K_2O$	0.08 %	7.67 %
$Na_2O$	-	1.78 %
$MgO$	-	1.33 %
$MnO$	0.06 %	0.18 %
$ZrO_2$	0.04 %	0.014 %
$Cr_2O_3$	0.03 %	0.04 %
$NiO$	0.03 %	-
$ZnO$	0.03 %	0.12 %
$Ga_2O_3$	0.01 %	-
$SrO$	0.01 %	0.08 %
$Br$	0.003 %	-

The X-ray Diffraction (XRD) patterns (Figure 1) complement the XRF findings by providing detailed information about the crystalline phases present in the KRC and ore tailings. The XRD analysis of KRC (Figure 1a) reveals the presence of several key minerals, including nacrite, magnetite, calcite, and titania. Nacrite, a kaolin group mineral, is consistent with the high alumina content found in the XRF data (31.46%). This clay mineral contributes to the plasticity of KRC, allowing it to form well-structured ceramics after sintering[19]. Magnetite, which correlates with the high iron oxide concentration in KRC, indicates the presence of iron-rich phases that further enhance the material's structural properties[20]. The small amounts of calcite ( $CaCO_3$ ) and titania ( $TiO_2$ ) are also significant, as they not only improve the overall durability but also influence the ceramic's resistance to marine conditions by contributing to its chemical stability[21].

For the ore tailings (Figure 1b), the XRD pattern shows a different set of minerals, including albite, aluminum phosphate, saponite, and vermiculite. The presence of albite, a sodium feldspar, is in line with the high  $Na_2O$  content (1.78%) observed in the XRF results. Albite plays an important role in the fluxing properties of the material, reducing the sintering temperature and enhancing the formation of a dense ceramic matrix[19]. The appearance of aluminum phosphate is also notable, as phosphate compounds can contribute to the formation of stable ceramic structures and may offer ecological benefits in artificial reef applications by promoting bioactivity[22]. The phyllosilicate minerals saponite and vermiculite, both present in the ore tailings, are known for their high cation-exchange capacities, which could enhance the ecological performance of the artificial reef by providing surfaces for marine organisms to colonize and thrive[23].

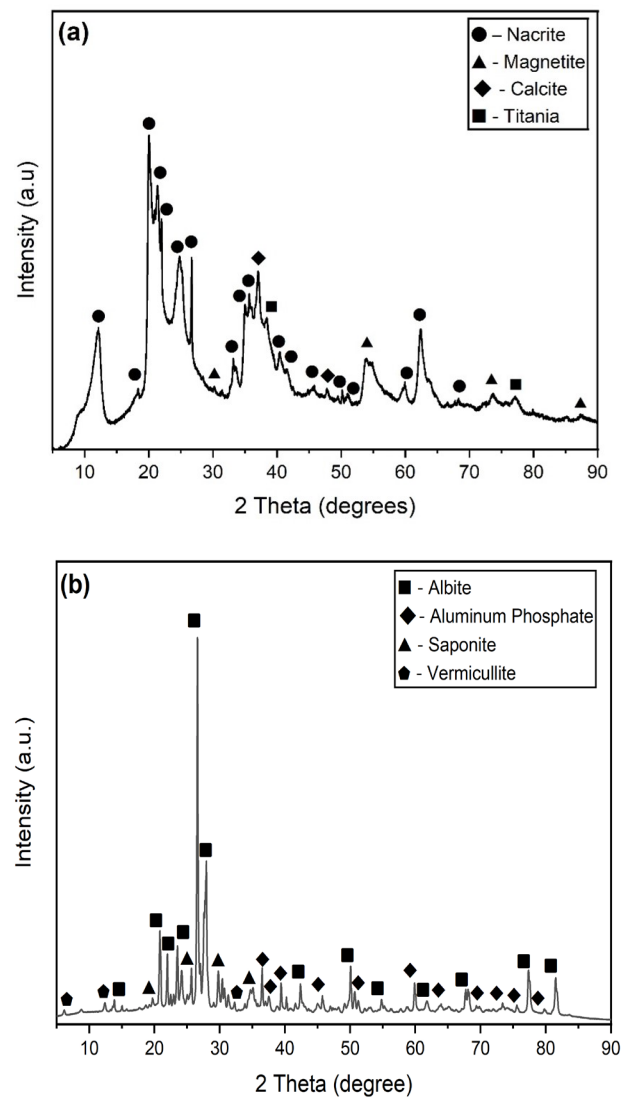


**Figure 1** X-ray diffraction pattern of a) Kauswagan Red Clay and b) Ore Tailings

The thermal behavior of Kauswagan Red Clay (KRC) and ore tailings was evaluated using thermogravimetric analysis (TGA) and differential thermal analysis (DTA), as shown in Figure 2. In the case of KRC (Figure 2a), the TGA curve shows a significant weight loss that occurs in several stages. The initial weight loss, starting at around 91°C and peaking near 251°C, is attributed to the evaporation of physically adsorbed water and the removal of hydroxyl groups from the clay minerals, which is typical for kaolinite and related alumina-silicate minerals[24]. The DTA curve supports this interpretation with an endothermic peak at 91°C, corresponding to the dehydration process. As the temperature increases, another endothermic peak at around 448°C is observed in the DTA curve, corresponding to the dehydroxylation of kaolinite, which leads to the formation of metakaolinite[25].

This dehydroxylation process is accompanied by further weight loss, as reflected in the TGA curve, which stabilizes at higher temperatures.

The particle size analysis of the materials is shown in Table 2.

**Table 2** Particle Size Analysis

Property	Material	
	KRC	Ore Tailings
<b>Mean Volume Diameter</b>	20.85	72.35
<b>Peak (µm)</b>	24.16	68.68

The table presents a comparison of particle size characteristics between two materials: KRC and Ore Tailings. The Mean Volume Diameter (MVD), which indicates the average particle size based on volume, is 20.85 µm for KRC and 72.35 µm for Ore Tailings. Similarly, the Peak Size, representing the most frequent particle size, is 24.16 µm for KRC and 68.68 µm for Ore Tailings.

These differences in particle size can significantly impact their suitability as materials for artificial ceramic coral reef structures. Smaller particle sizes, like those of KRC, provide a higher surface area per unit volume, which can enhance the binding properties and result in a denser, more compact structure. This characteristic can promote better adhesion and support the growth of marine organisms, mimicking the texture and microhabitats of natural coral reefs.

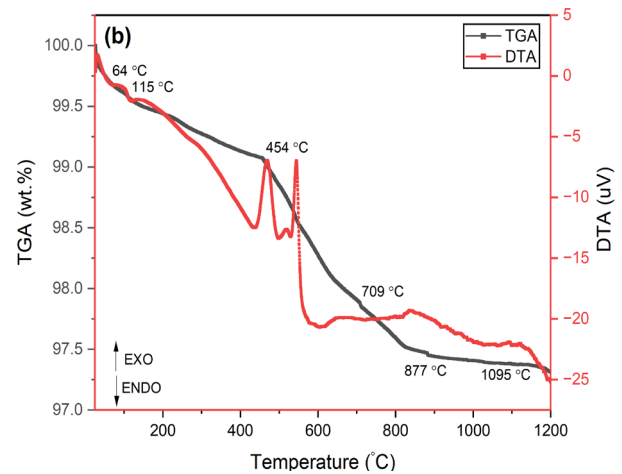
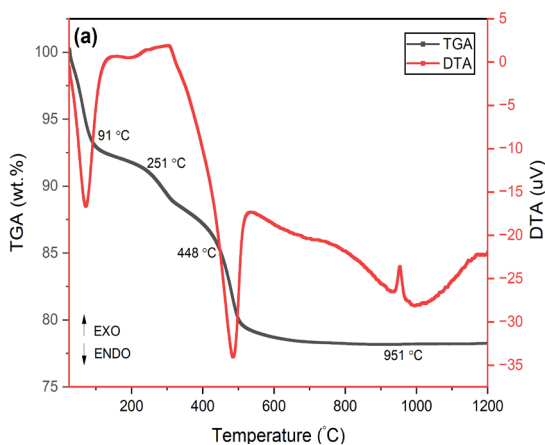


**Figure 2** TGDTA of a) Kauswagan Red Clay and b) Ore Tailings

On the other hand, larger particles, like those found in Ore Tailings, create a more porous structure. Increased porosity can enhance water flow and nutrient exchange, which is beneficial for marine life colonization and the settlement of coral larvae. However, too much porosity might compromise the structure's mechanical strength and durability, especially in turbulent marine environments.

At higher temperatures, a sharp exothermic peak at 951°C is observed in the DTA curve, indicating the crystallization of new phases. This corresponds to the transformation of meta kaolinite into mullite and other crystalline phases, as confirmed by the XRD analysis[26]. The formation of mullite is crucial for enhancing the mechanical properties and thermal stability of ceramic materials, making KRC a promising candidate for sintered ceramic products intended for high-temperature applications or underwater deployment.

For ore tailings (Figure 2b), the thermal profile also shows distinct weight loss stages but with some differences compared to KRC. The initial weight loss begins at a lower temperature, around 64°C, and continues until about 115°C, corresponding to the removal of adsorbed water. This is followed by a more pronounced endothermic peak at 454°C, which likely corresponds to the decomposition of hydroxylated minerals, such as vermiculite or saponite, as suggested by the XRD analysis[27]. These minerals decompose at lower temperatures compared to kaolinite, which explains the shift in the dehydroxylation process.

As the temperature rises, the DTA curve of ore tailings exhibits several exothermic peaks, the most prominent being at 709°C and 877°C. These peaks are associated with the phase transformation of silicates and the crystallization of new phases, potentially including aluminosilicates and iron oxides, as identified in the XRD results[28]. The final exothermic peak at 1095°C corresponds to the formation of crystalline phases such as spinel and aluminum phosphates, which contribute to the material's mechanical strength and potential bioactivity for artificial reef applications[22].

The thermal behavior of both materials highlights their potential for high-temperature applications. KRC exhibits better thermal stability due to its higher dehydroxylation and crystallization temperatures, while the ore tailings show lower temperature decomposition, which could influence the final properties of sintered products. These thermal properties, when combined with the chemical compositions observed in the XRF and XRD analyses, suggest that KRC and ore tailings can be used in complementary ways to optimize the performance of ceramic materials, balancing strength, porosity, and ecological benefits for marine applications.

After the initial material characterizations, the test bars were fabricated based on the ultimate proximate method, sample test bars are shown in Figure 3.



**Figure 3** Fabricated Sample Test Bars

As shown in Figure 4, the flexural strength of the material increases significantly with higher sintering temperatures, as seen in the progression from 10.7 MPa at 850°C to 66.75 MPa at 1135°C.

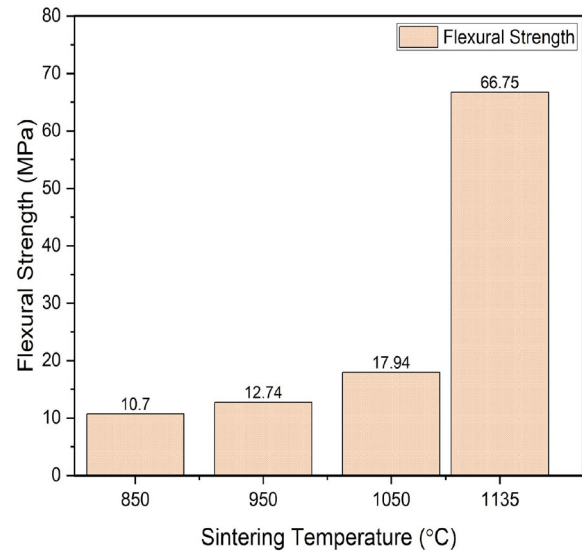


**Figure 4** Flexural Strength of Sample Test bars at different sintering temperatures

At 850°C, the flexural strength is relatively low, indicating incomplete densification or weak bonding between particles. As the sintering temperature increases to 950°C and 1050°C, the flexural strength rises to 12.74 MPa and 17.94 MPa, respectively, suggesting that particle bonding improves with increased temperature, likely due to enhanced diffusion and material consolidation [11]. Finally, at 1135°C, the flexural strength reaches a peak value of 66.75 MPa, which may be attributed to nearly complete densification, minimizing porosity and maximizing the strength of the ceramic body [12].

This trend reflects the general behavior of ceramics, where higher sintering temperatures lead to improved mechanical properties due to enhanced material cohesion [13].

The physical characteristics of the sample test bars were analyzed after drying and firing at different temperatures. The graph in Figure 5 shows the relationship between sintering temperature and the physical properties of the material, specifically apparent porosity, bulk density, and water absorption. As the sintering temperature increases from 850°C to 1135°C, there is a significant decrease in both apparent porosity and water absorption. Apparent porosity drops from around 35% at 850°C to below 10% at 1135°C, while water absorption similarly decreases from approximately 16% to about 11%. This reduction can be attributed to the densification of the material at higher sintering temperatures, leading to fewer voids and, therefore, lower porosity and water uptake [10-12, 29].

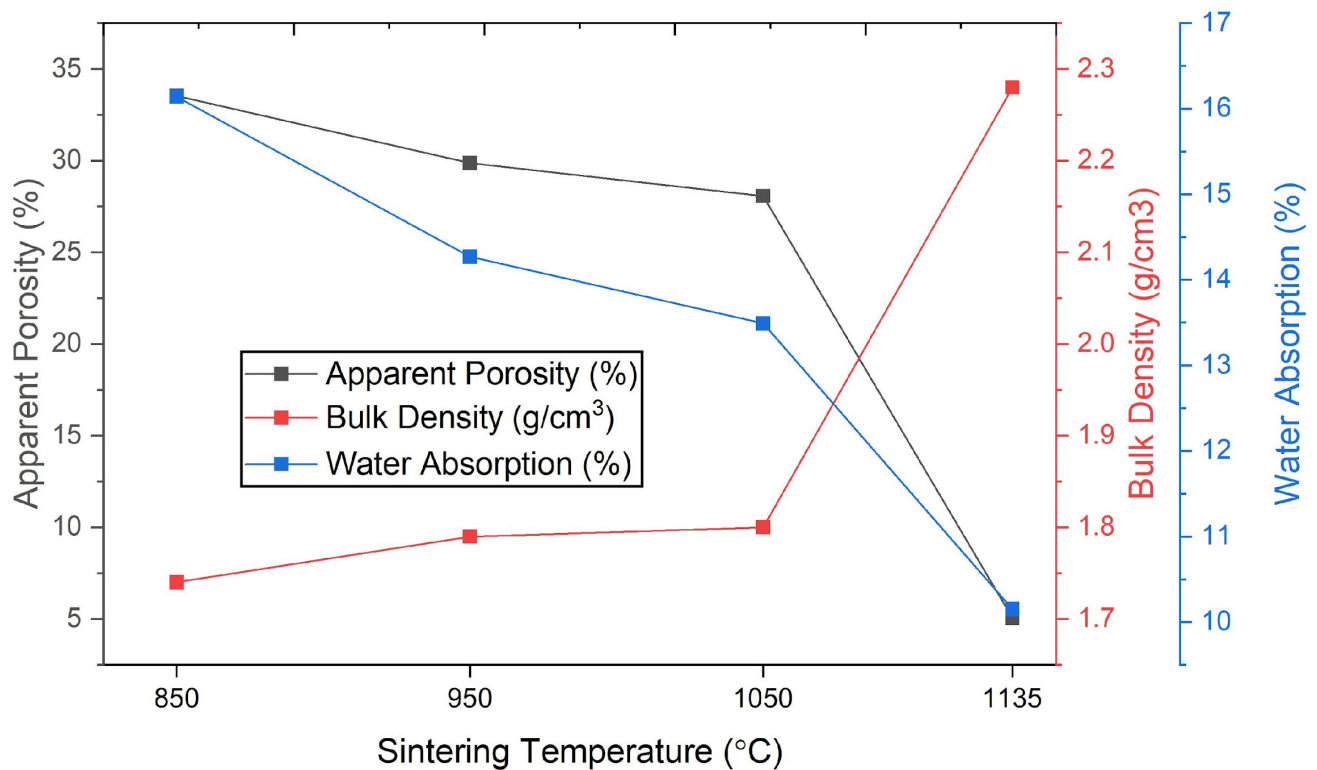


Figure 5 Physical Properties of Sample Test bars at different sintering temperatures

Conversely, bulk density shows an increasing trend with temperature, starting at about 1.7 g/cm<sup>3</sup> at 850°C and reaching a peak of 2.3 g/cm<sup>3</sup> at 1135°C. This increase in bulk density is consistent with the reduction in porosity, as higher temperatures promote particle rearrangement and compaction, resulting in a denser material structure[30]. The material becomes more compact and less porous, making it suitable for applications requiring durability and low permeability, such as artificial reef structures[14]. The data indicate that increasing the sintering temperature enhances the material's physical properties by reducing porosity and water absorption while increasing bulk density.

These changes suggest that the material becomes more compact and less permeable at higher temperatures, which is advantageous for applications like artificial reef structures where low porosity and water absorption are critical for durability and resistance to degradation in marine environment.

After 4 weeks of deployment, the 4 sample test bars per temperature were evaluated for bio-compatibility in terms of determined or found organism on the test bars during deployment, the process of determinations and assessment were conducted by graduate students of marine biology of Mindanao State University – Iligan Institute of Technology. The determined organisms are shown below in Figure 6.

The biological evaluation of the test bars exposed to the marine environment revealed a correlation between sintering temperature and biofouling activity, as seen in the number of organisms attached to each sample. Sample Set 1, sintered at 1135°C, recorded the highest total number of organisms with 54. The types of organisms found included *Bivalve veliger*,

*Pteria sp.*, *Fish eggs*, and *Hexacotium sp.* The large number of attached organisms suggests that despite the high sintering temperature, which typically results in a denser and less porous material, the surface still provided favorable conditions for marine life to adhere and grow. The variety of organisms found on this sample also indicates that a diverse range of species can thrive in these conditions.

In contrast, Sample Set 2, sintered at 1050°C, recorded a total of 49 organisms, slightly lower than the 1135°C set. The organisms present on this set included *Discobis sp.*, *Gastropod veliger*, and *Fish eggs*, among others. Although the number of organisms was less than that on the 1135°C sample, this sample still supported a relatively high level of biofouling. The slight reduction in organism count may be attributed to changes in the surface properties of the material at a lower sintering temperature, such as increased porosity, which may have affected the attachment and survival of certain species.

Sample Set 3, sintered at 950°C, and Sample Set 4, sintered at 850°C, showed progressively lower numbers of organisms, with 35 and 33 organisms respectively. These samples contained organisms such as *Lioloma pacificum*, *Polypsiphonia sp.*, and *Oscillatoria sp.* The decreasing trend in organism count with lower sintering temperatures suggests that the surface characteristics created by these temperatures may not have been as conducive to organism attachment or survival. However, the presence of several types of organisms, including fish eggs, indicates that the material surfaces at these sintering temperatures still provided a suitable environment for marine life, albeit to a lesser extent than the higher sintered samples.

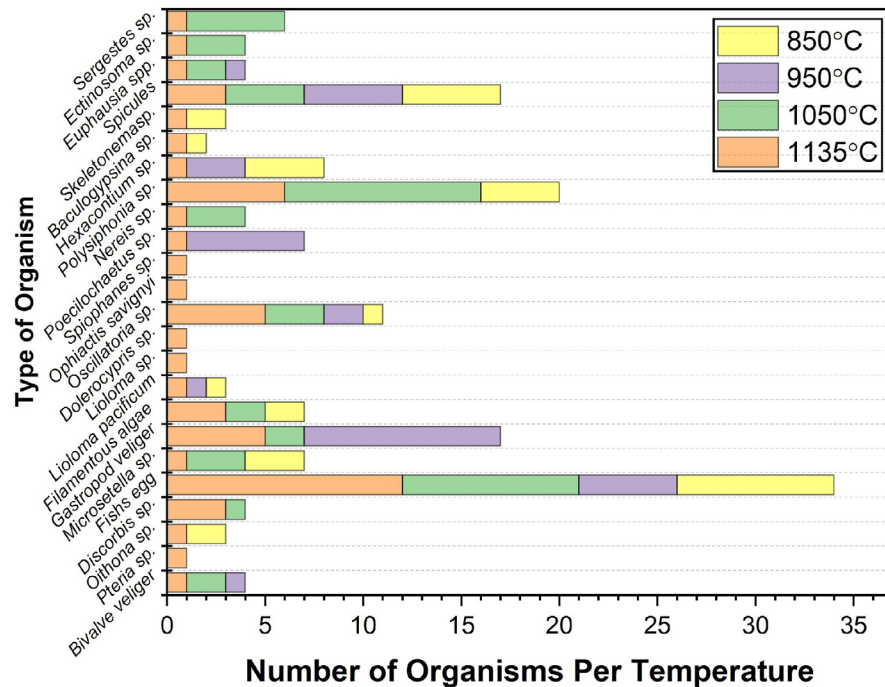


Figure 7 Type and Number of Marine Organisms of Sample Test bars at different sintering temperatures after deployment

#### 4.0 CONCLUSION

The study demonstrated a clear relationship between the sintering temperature of test bars and their biological performance when deployed in the marine environment. Among the four sintering temperatures examined, 1135°C yielded the highest biofouling activity, as indicated by the number and diversity of organisms that colonized the test bars. Lower sintering temperatures resulted in fewer attached organisms, with the 850°C sample showing the least amount of biofouling. These results suggest that the densification and surface characteristics of the materials, influenced by the sintering process, significantly affect the ability of marine organisms to adhere and thrive. The findings imply that higher sintering temperatures, which produce denser materials, may enhance biofouling activity, while lower sintering temperatures may limit organism attachment due to changes in surface porosity and texture. The study's insights are crucial for future applications in marine construction materials, where controlled biofouling or resistance to it may be desirable.

#### Acknowledgement

The researchers would like to acknowledge the Marine Biology Department, College of Science, for their assistance in identifying the algae and organisms found in the test bar samples during evaluation. They also extend their gratitude to the Lanao del Norte Divers Club, headed by Reynaldo R. Legaspi, together with club members Mr. Vicardy R. Aragon, Mr. Burth G. Dampas, Mr. Zigmund Israel Fernando, Mr. Juvim M. Miscala, and Mr. Eddie B. Sumile, for their support during the deployment of the test bars and ACCR samples in Linamon, Lanao del Norte.

#### Conflicts of Interest

The author(s) declare(s) that there is no conflict of interest regarding the publication of this paper

#### References

- [1] Q. He and B. R. Silliman, 2019 "Climate Change, Human Impacts, and Coastal Ecosystems in the Anthropocene," *Current Biology* 29(19): R1021-R1035. DOI: 10.1016/j.cub.2019.08.042.
- [2] R. Fisher *et al.*, 2015, "Species Richness on Coral Reefs and the Pursuit of Convergent Global Estimates," *Current Biology*. 25(4): 500-505, DOI: 10.1016/j.cub.2014.12.022.
- [3] W. Seaman and W. J. Lindberg, S. 2009. Edition, Ed. *Encyclopedia of Ocean Sciences (Artificial Reefs)*. Academic Press.
- [4] B. Vivier *et al.*, 2021. "Marine artificial reefs, a meta-analysis of their design, objectives and effectiveness," *Global Ecology and Conservation*. 27: e01538, DOI: 10.1016/j.gecco.2021.e01538.
- [5] M. A. Kalam, T. Mieno, and B. E. Casareto, 2018, "Development of Artificial Reefs Using Environmentally Safe Ceramic Material," *Journal of Ecosystem & Ecography*, 08(01): 1000253, DOI: 10.4172/2157-7625.1000253.
- [6] F. Pizarro Barraza *et al.*, 2024, "Unlocking the potential: Mining tailings as a source of sustainable nanomaterials," *Renewable and Sustainable Energy Reviews*, 202: 114665. DOI: 10.1016/j.rser.2024.114665.
- [7] H. Yu, I. Zahidi, M. F. Chow, D. Liang, and D. Ø. Madsen, 2024, "Reimagining resources policy: Synergizing mining waste utilization for sustainable construction practices," *Journal of Cleaner Production*, 464: 142795. DOI: 10.1016/j.jclepro.2024.142795.
- [8] P. Kinnunen, M. Karhu, E. Yli-Rantala, P. Kivikytö-Reponen, and J. Mäkinen, 2022, "A review of circular economy strategies for mine tailings," *Cleaner Engineering and Technology*, 8: 100499 DOI: 10.1016/j.clet.2022.100499.
- [9] S. Islam *et al.*, 2024. "Development of lightweight structural concrete with artificial aggregate manufactured from local clay and solid waste materials," *Heliyon*, 10(15): e34887. DOI: 10.1016/j.heliyon.2024.e34887.
- [10] M. L. Jalaluddin, U. A.-A. Azlan, M. W. A. Rashid, and N. Tamin, 2024, "Effect of sintering temperatures on the physical, structural

- properties and microstructure of mullite-based ceramics," *AIMS Materials Science*, 11(2): 243-255, DOI: 10.3934/mat.2024014.
- [11] S. Kitouni and A. Harabi, "Sintering and mechanical properties of porcelains prepared from algerian raw materials," *Cerâmica*, 57(344): 453-460, / 2011, DOI: 10.1590/s0366-69132011000400013.
- [12] N. B. Mustapa et al., 2023// "Effect of Sintering Mechanism towards Crystallization of Geopolymer Ceramic-A Review," *Materials (Basel)*, 16(11): 4103, DOI: 10.3390/ma16114103.
- [13] I. V. Matus, J. L. Alves, J. Góis, P. Vaz-Pires, and A. Barata da Rocha, 2024, "Artificial reefs through additive manufacturing: a review of their design, purposes and fabrication process for marine restoration and management," *Rapid Prototyping Journal*, 30(11): 87-122, DOI: 10.1108/rpj-07-2023-0222.
- [14] J. Huang, R. J. Lowe, M. Ghisalberti, and J. E. Hansen. 2024. "Wave transformation across impermeable and porous artificial reefs," *Coastal Engineering*, 189: 104488. DOI: 10.1016/j.coastaleng.2024.104488.
- [15] M. M. Yadollahi, A. Benli, and R. Demirboğa, 2015, "The effects of silica modulus and aging on compressive strength of pumice-based geopolymer composites," *Construction and Building Materials*. 94: 767-774, DOI: 10.1016/j.conbuildmat.2015.07.052.
- [16] A. M. Abyzov, 2019, "Aluminum Oxide and Alumina Ceramics (review). Part 1. Properties of Al<sub>2</sub>O<sub>3</sub> and Commercial Production of Dispersed Al<sub>2</sub>O<sub>3</sub>," *Refractories and Industrial Ceramics* 60(1): 24-32, DOI: 10.1007/s11148-019-00304-2.
- [17] J. Y. Y. Andji, A. A. Toure, G. Kra, J. C. Jumas, J. Yvon, and P. Blanchart, 2009, "Iron role on mechanical properties of ceramics with clays from Ivory Coast," *Ceramics International*, 35(2): 571-577, DOI: 10.1016/j.ceramint.2008.01.007.
- [18] L. Graziani, E. Quagliarini, F. Bondioli, and M. D'Orazio, 2014, "Durability of self-cleaning TiO<sub>2</sub> coatings on fired clay brick façades: Effects of UV exposure and wet & dry cycles," *Building and Environment*. 71: 193-203. DOI: 10.1016/j.buildenv.2013.10.005.
- [19] N. Kumari and C. Mohan, 2021. "Basics of Clay Minerals and Their Characteristic Properties," in *Clay and Clay Minerals*, G. M. D. Nascimento Ed.,
- [20] M. D. Nguyen, H.-V. Tran, S. Xu, and T. R. Lee, 2021. "Fe<sub>3</sub>O<sub>4</sub> Nanoparticles: Structures, Synthesis, Magnetic Properties, Surface Functionalization, and Emerging Applications," *Applied Sciences*, 11(23): 11301, DOI: 10.3390/app112311301.
- [21] N. Boluda-Botella, M. D. Saquete, S. Martínez-Moya, C. A. Morales-Paredes, and J. M. Rodríguez-Díaz, 2024, "Analysis of Calcium Carbonate Scales in Water Distribution Systems and Influence of the Electromagnetic Treatment," *Water*. 16(11): 1554. DOI: 10.3390/w16111554.
- [22] S. V. Dorozhkin, 2022. "Calcium Orthophosphate (CaPO<sub>4</sub>)-Based Bioceramics: Preparation, Properties, and Applications," *Coatings*, 12(10): 1380. DOI: 10.3390/coatings12101380.
- [23] C. Elmi, 2023, "Physical-Chemical Properties of Nano-Sized Phyllosilicates: Recent Environmental and Industrial Advancements," *Encyclopedia*. 3(4): 1439-1460, DOI: 10.3390/encyclopedia3040103.
- [24] S. Gu, X. Kang, L. Wang, E. Lichtfouse, and C. Wang, 2018, "Clay mineral adsorbents for heavy metal removal from wastewater: a review," *Environmental Chemistry Letters*. 17(2): 629-654, DOI: 10.1007/s10311-018-0813-9.
- [25] A. E. Kassa, N. T. Shibeshi, B. Z. Tizazu, and E. Guibal, 2022. "Characterization and Optimization of Calcination Process Parameters for Extraction of Aluminum from Ethiopian Kaolinite," *International Journal of Chemical Engineering*, 2022: 1-18, DOI: 10.1155/2022/5072635.
- [26] S. Lee, Y. J. Kim, and H. S. Moon, 2004. "Phase Transformation Sequence from Kaolinite to Mullite Investigated by an Energy-Filtering Transmission Electron Microscope," *Journal of the American Ceramic Society*. 82(10): 2841-2848, DOI: 10.1111/j.1151-2916.1999.tb02165.x.
- [27] K. Yin, H. Hong, G. J. Churchman, Z. Li, W. Han, and C. Wang, 2014, "Characterisation of the hydroxy-interlayered vermiculite from the weathering of illite in Jiujiang red earth sediments," *Soil Research*, 52(6): 505–514. DOI: 10.1071/sr14014.
- [28] F. Fajaro, H. Setyawan, A. Nur, and I. W. Lenggono, 2013. "Thermal stability of silica-coated magnetite nanoparticles prepared by an electrochemical method," *Advanced Powder Technology*. 24(2): 507-511, DOI: 10.1016/j.apt.2012.09.008.
- [29] X. Zhao, Q. Liu, J. Yang, W. Zhang, and Y. Wang, 2018. "Sintering Behavior and Mechanical Properties of Mullite Fibers/Hydroxyapatite Ceramic," *Materials (Basel)*, 11(10): 1859. DOI: 10.3390/ma11101859.
- [30] Y. Chen, N. Wang, O. Ola, Y. Xia, and Y. Zhu, 2021. "Porous ceramics: Light in weight but heavy in energy and environment technologies," *Materials Science and Engineering: R: Reports*, 143: 100589. DOI: 10.1016/j.msere.2020.100589.